Journal of Neuroscience Methods 197 (2011) 333–339

Contents lists available at ScienceDirect

Journal of Neuroscience Methods

journal homepage: www.elsevier.com/locate/jneumeth

Functional network analysis reveals differences in the semantic priming task

Stefan Schinkel[a,*], Gorka Zamora-López[a,b], Olaf Dimigen[c], Werner Sommer[c], Jürgen Kurths[a,d]

[a] Department of Physics, Humboldt University at Berlin, Germany
[b] Bernstein Center for Computional Neuroscience, Berlin, Germany
[c] Department of Psychology, Humboldt University at Berlin, Germany
[d] Potsdam Institute for Climate Impact Research (PIK), Germany

ARTICLE INFO

Article history:
Received 3 November 2010
Received in revised form 26 January 2011
Accepted 22 February 2011

Keywords:
Functional networks
Semantic priming
N400

ABSTRACT

The recent years have seen the emergence of graph theoretical analysis of complex, functional brain networks estimated from neurophysiological measurements. The research has mainly focused on the graph characterization of the resting-state/default network, and its potential for clinical application. Functional resting-state networks usually display the characteristics of small-world networks and their statistical properties have been observed to change due to pathological conditions or aging.

In the present paper we move forward in the application of graph theoretical tools in functional connectivity by investigating high-level cognitive processing in healthy adults, in a manner similar to that used in psychological research in the framework of event-related potentials (ERPs). More specifically we aim at investigating how graph theoretical approaches can help to discover systematic and task-dependent differences in high-level cognitive processes such as language perception. We will show that such an approach is feasible and that the results coincide well with the findings from neuroimaging studies.

1. Introduction

The brain and its network structure are one of the most challenging research subjects in (cognitive) neuroscience. The recent past saw substantial developments of tools to analyze, describe and statistically classify networks by means of graph theory. It has been demonstrated that to a large extent graph theoretical measures could already be applied to brain networks either on anatomical and functional levels revealing characteristic network features and different organizational scales (Bullmore and Sporns, 2009). The research in functional connectivity with human subjects has mainly focused on the investigation of properties of the resting-state/default network, i.e. when participants are not performing any particular task (Stam and Reijneveld, 2007). Resting state networks display *small-world* characteristics, which have been observed to change in pathological conditions (Stam et al., 2006; Supekar et al., 2008) or during aging (Micheloyannis et al., 2009; Fair et al., 2009; He and Evans, 2010). These observations might have clinical applications.

In the present paper we advance in the research on functional brain connectivity by applying graph theoretical tools to high-level cognitive processes in healthy adults. We aim to explore whether graph-theoretical tools can be used to identify task-dependent differences in the functional brain activity from neurophysiological measurements. Given electroencephalographic (EEG) data recorded during two different experimental conditions, we investigate whether their corresponding functional networks are significantly different of each other. The purpose of this paper is twofold – firstly we want to investigate whether we can replicate (classical) findings of ERP research using a graph theoretical approach and secondly, whether such measurements can provide additional information that have not been investigated by classical ERP analysis.

In comparison to other studies of functional connectivity, this paper features two main technical novelties. (i) We use joint recurrence plots (JRPs), to estimate dynamical inferences (functional links) between the individual nodes of the network, in our case the electrodes used for recording the EEG. This allows us to study the cerebral activity in the sensor (electrode) space while being less prone to artifacts caused by volume conduction. (ii) We do investigate network characteristics over a wide range of thresholds rather than for a fixed threshold, scanning through the levels of organization of the underlying network, ranging from full synchronization to complete segregation.

The main result of our study is that we can indeed replicate findings from functional imaging studies that convincingly argue that the process under investigation, the N400 component (see Section 2.3), does not reflect an isolated process but rather the sum of multiple, distributed processes.

The paper is organized as follows: the next section will familiarize the reader with some basic concepts of functional network analysis. The semantic priming experiment will be outlined in Sec-

* Corresponding author. Tel.: +49 331 977 2013.
E-mail address: schinkel@physik.hu-berlin.de (S. Schinkel).

0165-0270/$ – see front matter © 2011 Elsevier B.V. All rights reserved.
doi:10.1016/j.jneumeth.2011.02.018

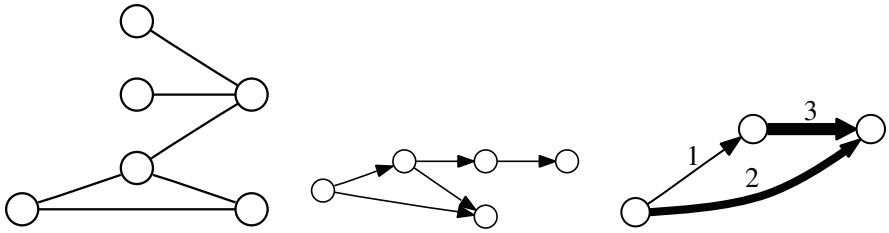

(a) Undirected and unweighted graph (b) Directed and unweighted graph (c) Directed and weighted graph

Fig. 1. Examples of networks: an undirected network (a) states only the presence of connections (links) between elements (nodes) of the network, a directed network (b) also provides a direction to that connection. Furthermore, a weighted network (c) also quantifies the strength of that connection.

tion 2.3. After presenting the key results in Section 3, we will conclude with a short discussion and an outlook.

2. Materials and methods

2.1. Complex networks

A network is, in the most general definition, a set of elements (nodes or vertices) with connections (links or edges) between them (Boccaletti et al., 2006; Newman, 2003; Costa et al., 2007; Arenas et al., 2008).

The links between the individual elements of a network can be *undirected*, indicating that there is a symmetric connection between two elements (Fig. 1a), or they can be *directed*, indicating the presence of asymmetry in the interaction between the nodes (Fig. 1b). Further, the links can be *weighted* and quantify the strength of the connection (Fig. 1c). Sometimes, the nodes and the links represent physical entities such as a set of computers and the cables connecting them, or the axonal connections between nerve cells. Links can, however, also represent more abstract features, e.g. college students who belong to the same fraternity, or the level of synchronization between two dynamical systems. Real networks derived from empirical data are usually termed *complex* because they are neither random nor regular, but possess some degree of organization which is not trivially observable.

A network of N nodes can be represented by a square matrix A, called adjacency matrix, of size $N \times N$. Its elements $A_{ij} = 1$ if there is a link connecting node i to node j. If there is no link between the two nodes, then $A_{ij} = 0$. In undirected networks A is symmetric.

The framework of graph theory includes a set of statistical descriptors which permit to uncover properties of networks at different scales of organization. The density of the network ρ, is the ratio of existing links to the number of all possible links. The degree of a node i, k_i is the number of links that i makes to other nodes, also referred to as the *neighbours* of node i. The average degree $\langle k \rangle$ is the average number of connections of the nodes within the network.

In networks, the distance between two nodes i and j is quantified as the number of links crossed to travel from one to another. If there is a link $i \rightarrow j$ ($A_{ij} = 1$) then the distance $d_{ij} = 1$. If there is no link between them, but it is possible to travel through another node s such that the path $i \rightarrow s \rightarrow j$ is possible, then the distance $d_{ij} = 2$, and so on. The average pathlength l is the average of all pairwise distance, $l = \langle d_{ij} \rangle$. Another important measure, the clustering coefficient C, characterizes the cohesiveness of the nodes. It terms of social networks, it captures the observation that two persons are more likely to be friends if they have a common friend. Formally, the clustering coefficient denotes the ratio between the number of triangles present in the network, and the number of possible triangles that could be formed. If the number of triangles is denoted by $N(\triangledown)$, and $N(\vee)$ is the number of connected triplets, then the clustering coefficient is quantified as: $C = 3 \times N(\nabla)/N(\vee)$. The factor accounts for the fact that each triangle contains three connected triplets.

2.2. Functional network estimation from neurophysiological data

In order to estimate functional networks from a time-series of measured data two key steps are required (Fig. 2). First, the dynamical inferences between all pairs of nodes have to be computed and summarised into a similarity or association matrix (Fig. 2b). The pairwise similarity can be quantified by classical statistical measures, e.g. linear cross-correlation or more advanced measures based on information theory, such as Granger causality (Granger, 1969) or partial directed coherence (Baccala and Sameshima, 2001). In the second step a threshold is applied to this matrix in order to conserve only the relevant connections/links giving rise to a binary network described by the adjacency matrix (Fig. 2c). This is a non-trivial step as there are no general guidelines on how to choose the threshold. In some studies a threshold is fixed and applied to all the networks (e.g. Fair et al., 2009) and in other studies the threshold is adapted such that all resulting functional networks all have the same number of links (e.g. Schindler et al., 2008). Once the adjacency matrix is derived, graph analysis measures can be applied to uncover its topological organization.

In the following we review this process in closer detail.

2.2.1. Defining dynamical similarity

Linear cross-correlation (Hogg et al., 1959) is usually the baseline criterion to evaluate the level of dynamical similarity between two time-series. But it may not be the optimal measure of similarity for the application at hand. In a typical EEG/ERP setup the distance between the electrodes is rather small, in the range of a few centimetres. In a high-resolution setup using 126 or even more electrodes, the distance sometimes is only a few millimetres. Due to the spatial proximity and volume conduction the cross-correlation between the neighbouring electrodes may yield very high correlation values. It will therefore be very difficult to decide whether the measured correlation is simply due to spatial proximity or does indeed capture a functional relationship. Unfortunately, measures quantifying true functional relationships like Granger causality or partial directed coherence on the other hand, are not feasible for the signals of the electrodes in an EEG experiment (sensor space) as volume conduction counteracts their application. Those measures should be only applied in the source space, i.e. the estimated sources of neural activity, derived from source localisation routines.

Therefore we here used a method defining the similarity matrix based on a recurrence analysis of time series (Marwan et al., 2007). Recurrence-based approaches have recently been shown to be a suitable tool for the analysis of EEG data in general (Komalapriya et al., 2009) and ERP data in particular (Schinkel et al., 2007, 2009a,b), because recurrence-based analysis is capable to cope with rather short, noisy and instationary time series.

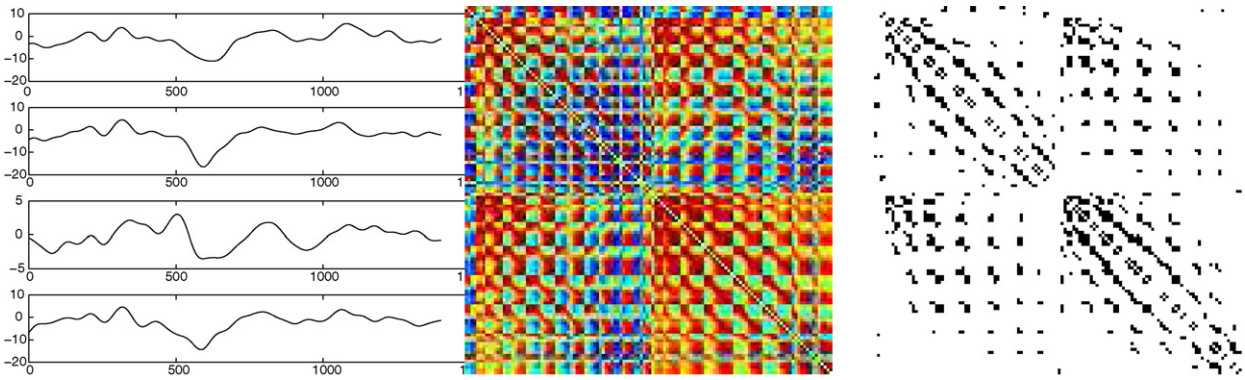

Fig. 2. The basic procedure for estimation of networks from time series. The pair-wise similarity of all measured time series (a) is computed and provides an association or similarity matrix (b). By applying a threshold to such an association matrix a binary adjacency matrix is estimated (c). This adjacency matrix is then used to compute statistical properties of the network.

For the estimation of the similarity matrices, we used joint recurrence plots (JRPs) which evaluate the simultaneous occurrence of recurrences in two systems and provide a generalisation of cross-correlation. A JRP is the Hadamard product of two recurrence plots (RPs):

$$\mathbf{RP}_{i,j} = \Theta(\varepsilon_x - ||x_i - x_j||), \quad i,j = 1,\ldots,n \tag{1}$$

An RP captures the recurrence properties of a single time series, such that $\mathbf{RP}_{i,j} = 1$ if the difference between the values at the time points x_i and x_j is less than a chosen recurrence threshold ε, otherwise $\mathbf{RP}_{i,j} = 0$. A JRP is a multivariate extension of RPs that captures the joint recurrence behaviour of two time series:

$$\mathbf{JRP}_{i,j} = \Theta(\varepsilon_x - ||x_i - x_j||) \cdot \Theta(\varepsilon_y - ||y_i - y_j||), \quad i,j = 1,\ldots,n \tag{2}$$

where x and y are the individual time series of length n at two nodes (electrodes) x and y. Θ is the Heaviside step function and ε is the recurrence threshold or the recurrence criterion.

A joint recurrence $\mathbf{JRP}_{i,j} = 1$ is only given if $\Theta(\varepsilon_x - ||x_i - x_j||) = 1 \wedge \Theta(\varepsilon_y - ||y_i - y_j||) = 1$, that is, if both time series recur simultaneously. The amount of joint recurrences gives an estimation of how similar the dynamical behaviour of two time series is.

For our analysis we use JRPs and a recurrence threshold criterion which ensures that all columns of the individual RPs have the same number of points. For all combinations of channels c_i the JRP_{c_i,c_j} were constructed and the joint recurrence rate JRR was calculated as:

$$\mathrm{JRR} = \frac{1}{N^2}\sum_{i,j=1}^{N}\mathbf{JRP}_{i,j} \tag{3}$$

This approach has the advantage, that it can assess the similarity between channels to a larger extent than linear measures and is less prone to spurious similarities as the dynamical behaviour is considered (Romano et al., 2005).

To cross-validate whether the findings would be obtainable with correlations as well, we also calculated dynamical similarities using linear correlation between electrodes.

2.2.2. Threshold selection

The selection of an appropriate threshold ε that is used to extract an adjacency matrix from the similarity matrix for the subsequent analysis is far from trivial. The chosen threshold crucially impacts the network statistics as shown in Table 1. It is usually difficult to decide, which threshold best reflects the network properties.

Table 1
Dependence of key network measures on the threshold ε applied to the similarity/association matrix: ρ is the network density, $\langle k\rangle$ is the average degree, l is the average pathlength, and C is the average clustering coefficient. The association matrix was computed from high-resolution EEG data recorded in the semantic priming experiment (Section 2.3).

ε	ρ	$\langle k\rangle$	l	C
0.5	0.2371	0.2352	1.7741	0.6592
0.6	0.0912	0.0905	3.8113	0.4931
0.7	0.0317	0.0315	10.6720	0.2740
0.8	0.0135	0.0134	59.0918	0.0862
0.9	0.0089	0.0088	112.5957	0.0238

Therefore we investigated the behaviour of the network over a range of thresholds. For each binary network extracted at different thresholds, we computed the number of network components. A network component is a subset of the nodes which are at finite graph distance, but have no links to nodes outside the network component (see Fig. 3).

For a very high ε in the functional network only those nodes with almost identical dynamical behaviour are connected. Hence, almost all nodes are disconnected from each other and there are as many network components as there are nodes. As ε decreases, more links are included into the functional network. This leads to

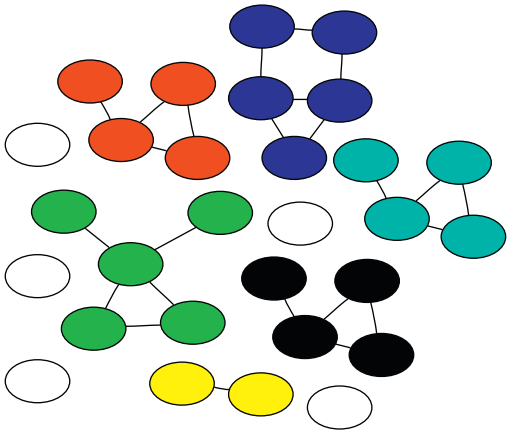

Fig. 3. The concept of network components: nodes that have links only among each other but not to nodes from another network component and are therefore filled with the same colour. Nodes that have no links are considered as network components of size one (blank nodes).

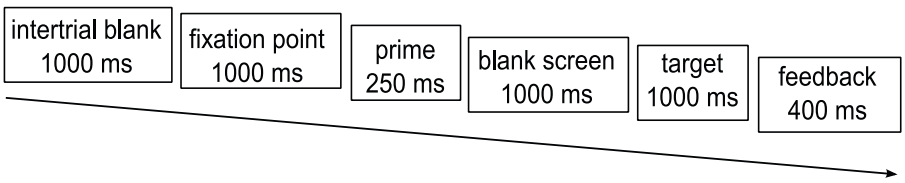

Fig. 4. Schematic of one experimental trial. The rather long interval between prime and target was chosen in order to avoid the inclusion of potentials evoked by the onset of the prime in the processing of the target-related EEG.

a merging of network components until only one network component remains. The interesting question here is how quickly this merging happens as the threshold is lowered, and if there is a difference in the network component formation between the functional networks derived from the two experimental conditions.

Notice that although the terminology is similar, a network component must not be confused with an ERP component, which denotes a particular spatio-temporal pattern in the recorded EEG data.

2.3. Semantic priming study

10 young adults (1 male and 9 female) aged 19–38 (mean 23.6; SD 5.4 years) participated in a semantic priming experiment. All were right-handed (mean handedness index: +98 according to Oldfield (1971)), monolingual native speakers of German and gave written consent to the experiment. Subjects received either payment or course credits. The EEG was recorded from 126 Ag/AgCl electrodes (impedances $\leq$5 kΩ) at a sampling rate of 1000 Hz using a BrainAmp DC amplifier (Brain Products GmbH, Munich, Germany). All electrodes were initially referenced to an electrode on the left mastoid (A1) and converted off-line to linked-mastoid reference. The EEG data was bandpass filtered from 1 to 30 Hz. Trials with artifacts or a wrong response were excluded from the analysis.

The subjects were presented with a prime word that was either a synonym of a following target word or an unrelated noun. The experimental setup was as follow, after a 1000 ms blank screen (inter-trial-interval) a fixation point appeared for 1000 ms, which was then replaced with the prime. The prime was presented for 250 ms follow by another blank screen (1000 ms) before the target was shown for 1000 ms. Finally a feedback screen was shown for 400 ms informing the subject if they where to slow or gave a wrong response. If the response was correct no explicit feedback was given (Fig. 4). We used the rather long stimulus onset asynchrony of 1000 ms in order to avoid the inclusion of potentials evoked by the onset of the prime in the processing of the target-related EEG.

The stimulus material was taken from Hohlfeld et al. (2004). In total subjects had to read 240 items, 120 in each condition. Subjects had to indicate by a button press with either the right or left hand, whether the presented word was synonymous or not. The response hand was changed midway during the experiment. The high degree of semantic relatedness of synonymous words as compared to the unrelated words strongly modulates N400 component. The N400 component reflects the retrieval of semantic word information from long term memory (Kutas and Federmeier, 2000) and its integration into the semantic context provided by the prime word. If this semantic retrieval and integration is easy as for synonymous words, the N400 amplitude is small, whereas it is large (about 5 μV) when there is no such context as in the case of unrelated prime words. Recent studies found that the N400 does not reflect the activity of a clearly localised brain system process but rather reflects the activity of distributed neuron ensembles that act as functional units (Pulvermüller, 1996, 2001). According to the literature all studies found effects involving the left middle temporal gyrus (MTG) but also other sources. For semantic priming manipulations inferior frontal effects are also reported, but there is less consistency in these effects as compared to the involvement of the MTG (see Lau et al., 2008, for a review).

For the network estimation and subsequent analysis we focused on two time windows. The first window (pre-stimulus window) ranging from 200 ms pre-stimulus to stimulus onset was chosen as a reference for the comparison (Fig. 5).

For the critical part of the analysis the data was response-locked. The subject's response, the button press participants had to provide, and not the stimulus onset was used to align the individual EEG segments (epochs). The window chosen here, the N400 window, ranges from 200 ms before response the button press until the response. This window captures the time of divergence of the

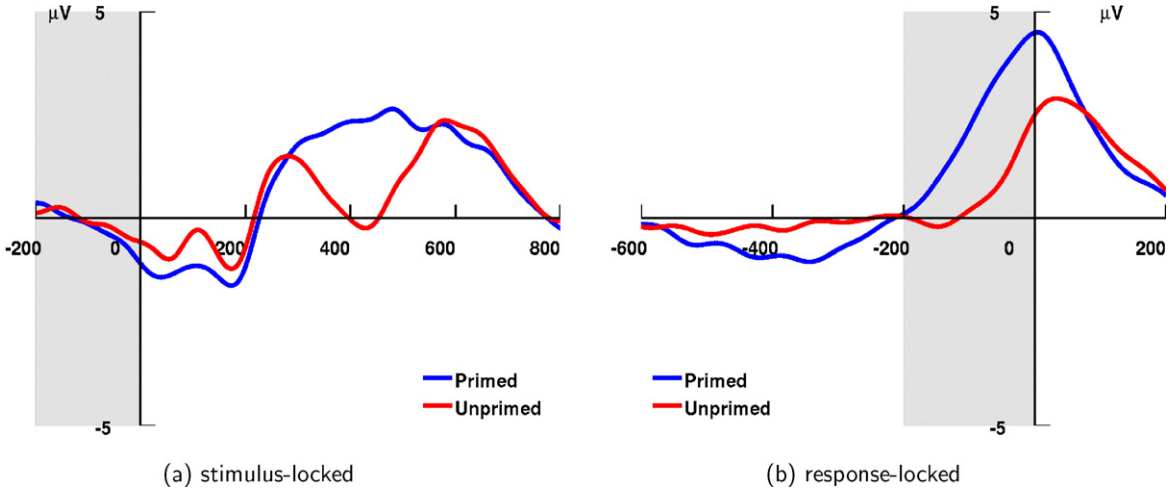

Fig. 5. Grand average ERPs locked to stimulus onset (a) and locked to the subject's response (b) at a centro-parietal site (CPZ). The two time windows considered in the analysis are highlighted in the plots. For the reference window we chose the 200 ms preceding the stimulus presentation, for the N400 window we used the 200 ms window immediately before the response (button press).

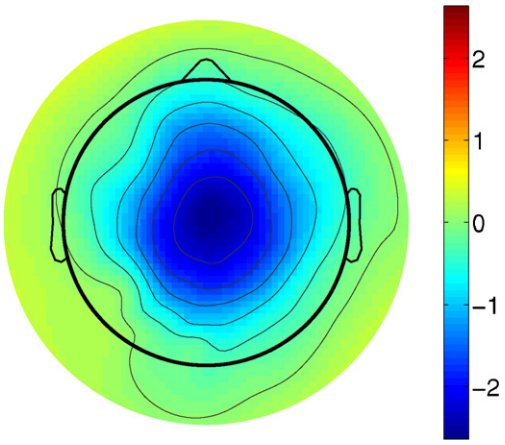

Fig. 6. Topology of the grand average ERP for the difference primed – unprimed condition in the N400 window, the same window that was subjected to the network component analysis (Fig. 7).

two ERPs waveforms (Fig. 6) until the response was given. For the functional network analysis we deliberately chose to lock the data to the subject's response, to counteract *latency jitter*. Latency jitter refers to the effect that the trial-to-trial variability can be considerably large which can distort the ERP waveform and potentially lead to broad, low-amplitude waveforms. Locking the data to the response thus effectively limits the impact of latency jitter.

We tested the following hypothesis: within the window immediately preceding the response, the experimental manipulation (primed × unprimed) should elicit a difference between both conditions that reflects the experimental manipulation. In contrast we should not be able to observe a difference in pre-stimulus window.

3. Results

The analysis was done on the averaged data. For each subject we averaged the EEG data within each condition and estimated the similarity matrix in the pre-stimulus and the N400 window.

For a first impression, we investigated whether a qualitative effect can be observed. Fig. 7 shows the colour-coded network components according to their distribution on the head. The primed and the unprimed condition clearly differ in qualitative terms. With primed items we observed a behaviour that is most adequately described as global synchronization where one large network component dominates the dynamics. The unprimed items (N400 condition) elicit a different and more complex behaviour. Here the network component structure is more elaborate, revealing a larger, lateralized network component along with several smaller network components.

We then investigated whether this effect is statistically significant. For this we computed the total number of network components in the networks while lowering the threshold from 1.0 to 0.5. During this process the network structure is bound to shift from one extreme state – total segregation – to the opposite extreme – global synchronization. For a threshold of 1, which requires identity of the nodes in order to be clustered together, all nodes form a cluster of their own, resulting in as many clusters as there are electrodes. This is the state of total segregation. The lower the threshold, the more nodes will be clustered together until only one single cluster remains. This is the state of global synchronization. This state can be understood as a kind of default or resting state in which no particular processing is dominant. This in turn means, that the higher the threshold at which this state emerges, the closer the underlying system, in our case the brain, is to the default state. As complexity emerges in-between those two states, it is of interest for our analysis, whether the path of this transition is different between the two conditions examined.

The analysis was performed using four functional networks extracted from the EEG data: a window of pre-stimulus data (200 ms previous to stimulus onset) in both conditions (primed and unprimed) and in the N400 windows of both conditions as described above. We find that the number of network components drops in both conditions and windows as the threshold is lowered. In the pre-stimulus window the decay rate of the number of clusters is similar in both conditions, primed and unprimed. A permutation test, the non-parametric counterpart of the classical *t*-test (Good, 2005), applied to the average number of network component across subjects, did not reveal any significant differences

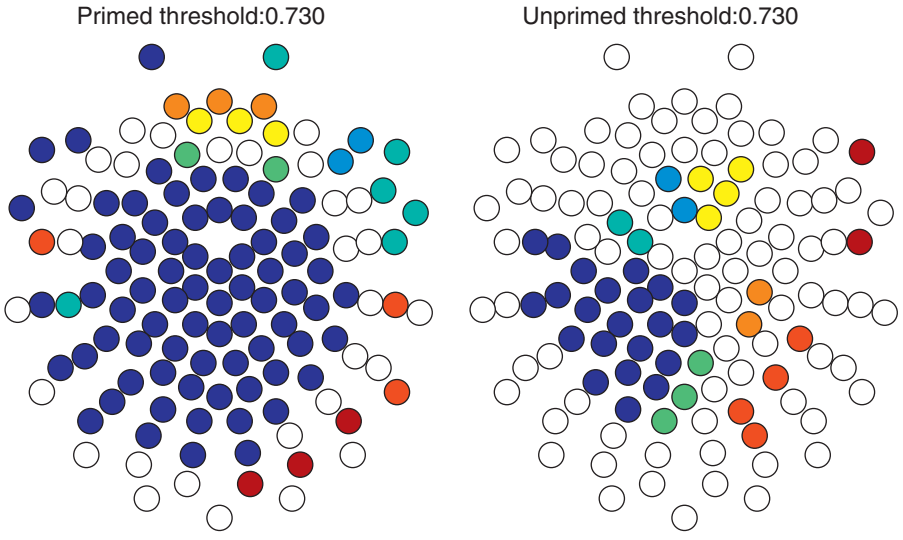

Fig. 7. Sample network component distribution for an exemplary subject in the N400 window for primed (left) and unprimed items (right). The threshold applied to the association matrix is the same in both conditions. Nodes (electrodes) in the same colour belong to the same network component. Nodes that form a distinct network component (i.e. a network component with only one member) are blank. It can be seen, that in the case of primed items a pattern of global synchronization emerges, where one network components "absorbs" all nodes in the network, whereas in the unprimed condition a larger, lateralized network component is present along with various smaller, distributed network components.

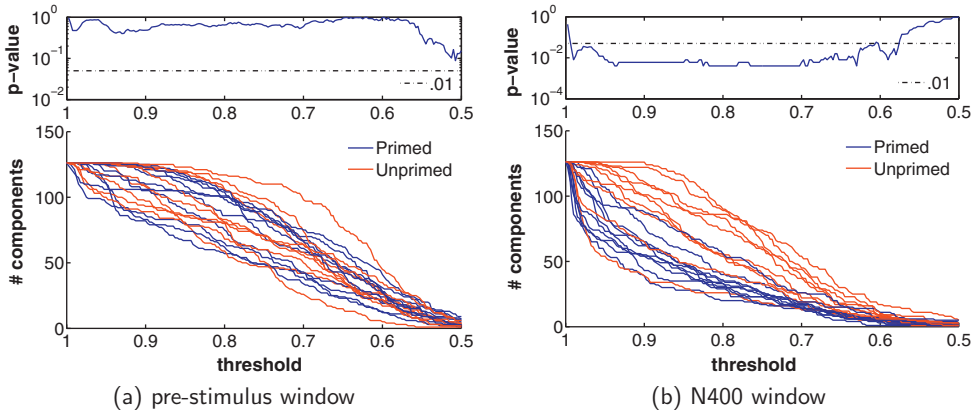

Fig. 8. The comparison for similarity matrices based on joint recurrence. Significant differences (upper panels) between the 2 conditions for a wide threshold range can be found in the N400 window (right panel), whereas no such differences are found in the pre-stimulus interval (left panel). The *p*-value of a sliding permutation test is plotted in the upper panels.

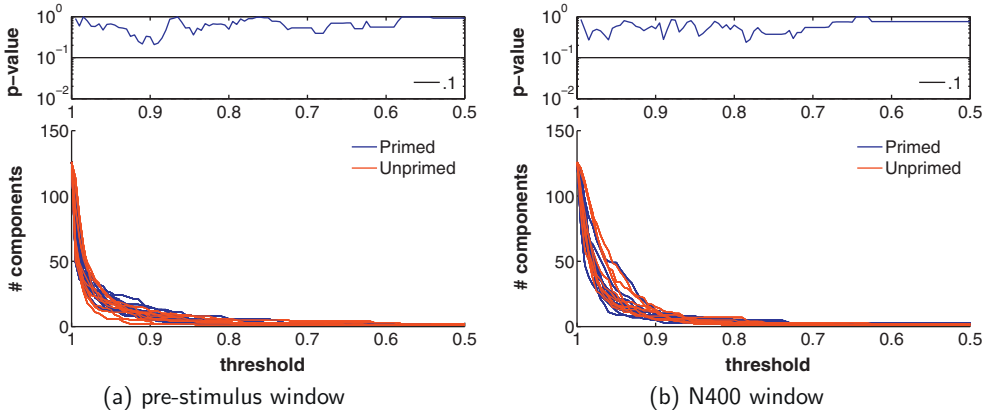

Fig. 9. The evolution of the number of network components found in the network vs. the threshold applied to the similarity matrix in the pre-stimulus window (left panel) and the N400 window (right panel). For definition of the similarity matrix linear cross-correlation was used. There is no significant difference in either of the windows.

between the primed and unprimed condition in the pre-stimulus interval for all thresholds considered (Fig. 8a).

In the N400 window the results are substantially different. The number of network components drops as the threshold is decreased. For unprimed items the decay of the number of network components is far slower than for primed items and less pronounced at higher thresholds. This can be argued to reflect the fact that in the primed condition the system is closer to the aforementioned default state, as the semantic processing is facilitated by the presentation of synonymous word. In the unprimed condition on the other hand, no such facilitation was provided by the prime. Therefore the semantic processing induces more cognitive load, which leads the system further away from the default state.

We again investigated whether this difference is significant by running a permutation test between the number of network components in both conditions at each threshold value for both time windows. And indeed, the difference in the number of network components is highly significant over a wide threshold range in the N400 window (Fig. 8b).

3.1. Benchmark comparison using linear correlation

In order to illustrate that the results of the analysis crucially depend on the measure chosen to define the association/similarity matrix, we ran a benchmark comparison. Analogous to the procedure shown in Fig. 8 we estimated the similarity matrix and then investigated the formation of network components as the threshold decreases. In this benchmark comparison we used linear correlation. Linear correlation is the standard measure to estimate similarities between two observations and was therefore chosen. Due to its nature, correlation can only capture linear dependencies in the data. The joint recurrence rate on the other hand also incorporates nonlinear aspects by investigating common characteristics in dynamic behaviour as expressed in the recurrence properties of the signals. Furthermore, as a recurrence approach it is less sensitive to nonstationarities and suitable for rather short data series.

Indeed it was found that linear correlation cannot be used to distinguish the primed from the unprimed condition in the same fashion the recurrence approach does (Fig. 9). We therefore argue that there are nontrivial, nonlinear interactions that are responsible for the results observed in Fig. 8.

4. Conclusion

The present study attempted to show the feasibility of defining functional networks on the basis of the similarity of recurrence plots by using data from a semantic priming experiment. Corresponding to the general knowledge about the processes underlying the N400, we found a distributed left-lateralized network component pattern in the case of an N400 response (unprimed items) whereas no such pattern could be observed for primed items. While the N400 seems to be constituted of a larger, lateralized network component along with various smaller additional network components, the primed items showed a pattern of global synchronization, which could be argued to reflect a kind of steady regime during the processing. Additional to this qualitative result, we could

also quantify this observation with a straight-forward statistical comparison, namely the number of the network components in the primed and unprimed cases, which verifies that this effect is stable across subjects.

Some points of our analysis deserve special highlighting. First of all, the criterion we used to construct the association matrix, the joint recurrence rate of two nodes/electrodes, seems to be capable of disentangling the truly functional relationships from the trivial relationships to a large extent. By using nonlinear methods we can investigate processes like the N400 in the electrode/sensor space where linear methods fail to do so and without the need for source reconstruction or other pre-processing methods that compensate for spatial smearing of the wave forms.

From a graph analytical point of view it has to be mentioned explicitly that our analysis has the advantage of circumventing the need of a priori selecting a threshold for the graph analysis. The selection of a threshold is usually rather arbitrary. By investigating the organization of the network over a range of thresholds we do not investigate a single network that might, in the worst case, have arisen only due to an inappropriate threshold and in general reflects only one aspect of the underlying data, but rather we investigate a series of possible networks. This has the great advantage that we can scan the range of possible functional and hierarchical organizational patterns the underlying network can represent.

Summarising, we have shown, that graph theoretical measures can be used to discriminate task-dependent differences during cognitive processing and additionally can provide information that goes beyond amplitude differences. Using a functional network approach in connection with an advanced data analysis tool to construct similarity/association matrices, we could find functional differences between two experimental conditions in the sensor-space. We were further able to show that this difference is stable over subjects and highly significant. Our findings indicate that there is some functional difference in the networks estimated from the EEG measurements. The results coincide well with the general understanding of the N400 in language processing in that it is a distributed process, that is, it involves multiple network. In contrast, the primed condition only shows the activity of a single network. Further applications of the proposed method could help to gain a deeper understanding of the functional networks underlying high level cognitive processes that are reflected in ERPs.

Acknowledgements

The authors would like to thank Romy Frömer and Ulrike Bunzenthal for assistance in running the experiments. This work has been supported by grants of the German Research Foundation (DFG) in the Research Group FOR 868 *Computational Modeling of Behavioral, Cognitive, and Neural Dynamics*. The software used for the analysis is available at http://www.agnld.uni-potsdam.de/~schinkel.

References

Arenas A, Díaz-Guilera A, Kurths J, Moreno Y, Zhou C. Synchronization in complex networks. Physics Reports 2008;469(3):93–153.
Baccala L, Sameshima K. Partial directed coherence: a new concept in neural structure determination. Biological Cybernetics 2001;84(6):463–74.
Boccaletti S, Latora V, Moreno Y, Chavez M, Hwang D. Complex networks: structure and dynamics. Physics Reports 2006;424(4–5):175–308.
Bullmore E, Sporns O. Complex brain networks: graph theoretical analysis of structural and functional systems. Nature Reviews Neuroscience 2009;10(3):186–98.
Costa LDF, Rodrigues FA, Travieso G, Boas PRV. Characterization of complex networks: a survey of measurements. Advances in Physics 2007;56:167–242.
Fair DA, Cohen AL, Power JD, Dosenbach NUF, Church JA, Miezin FM, et al. Functional brain networks develop from a "local to distributed" organization. PLoS Computational Biology 2009;5(5):e1000381.
Good P. Permutation, parametric and bootstrap tests of hypotheses. Springer series in statistics. Springer Verlag; 2005.
Granger C. Investigating causal relations by econometric models and cross-spectral methods. Econometrica: Journal of the Econometric Society 1969;37(3):424–38.
He Y, Evans A. Graph theoretical modeling of brain connectivity. Current Opinion in Neurology 2010;23(4):341.
Hogg R, Craig A, McKean J. Introduction to mathematical statistics. New York: Macmillan; 1959.
Hohlfeld A, Sangals J, Sommer W. Effects of additional tasks on language perception: an event-related brain potential investigation. Journal of Experimental Psychology: Learning, Memory, and Cognition 2004;30(5):1012–25.
Komalapriya C, Romano MC, Thiel M, Schwarz U, Kurths J, Simonotto J, et al. Analysis of high-resolution microelectrode EEG recordings in an animal model of spontaneous limbic seizures. International Journal of Bifurcation and Chaos 2009;19(2):605–17.
Kutas M, Federmeier K. Electrophysiology reveals semantic memory use in language comprehension. Trends in Cognitive Sciences 2000;4(12):463–70.
Lau E, Phillips C, Poeppel D. A cortical network for semantics: (de)constructing the N400. Nature Reviews Neuroscience 2008;9(12):920–33.
Marwan N, Romano MC, Thiel M, Kurths J. Recurrence plots for the analysis of complex systems. Physics Reports 2007;438(5–6):237–329.
Micheloyannis S, Vourkas M, Tsirka V, Karakonstantaki E, Kanatsouli K, Stam CJ. The influence of ageing on complex brain networks: A graph theoretical analysis. Human Brain Mapping 2009;30:200–8.
Newman MEJ. The structure and function of complex networks. SIAM Review 2003;45(2):167–256.
Oldfield R. The assessment and analysis of handedness: the Edinburgh inventory. Neuropsychologia 1971;9(1):97–113.
Pulvermüller F. Hebb's concept of cell assemblies an the psychophysiology of word processing. Psychophysiology 1996;33(4):317–33.
Pulvermüller F. Brain reflections of words and their meaning. Trends in Cognitive Sciences 2001;5(12):517–24.
Romano MC, Thiel M, Kurths J, Kiss IZ, Hudson J. Detection of synchronization for non-phase-coherent and non-stationary data. Europhysics Letters 2005;71(3):466–72.
Schindler KA, Bialonski S, Horstmann MT, Elger CE, Lehnertz K. Evolving functional network properties and synchronizability during human epileptic seizures. CHAOS 2008;18:033119.
Schinkel S, Marwan N, Dimigen O, Kurths J. Confidence bounds of recurrence-based complexity measures. Physics Letters A 2009a;373(26):2245–50.
Schinkel S, Marwan N, Kurths J. Order patterns recurrence plots in the analysis of ERP data. Cognitive Neurodynamics 2007;1(4):317–25.
Schinkel S, Marwan N, Kurths J. Brain signal analysis based on recurrences. Journal of Physiology – Paris 2009b;103(6):315–23.
Stam C, Reijneveld J. Graph theoretical analysis of complex networks in the brain. Nonlinear Biomedical Physics 2007;1(1):3.
Stam CJ, Jones BF, Nolte G, Breakspear M, Scheltens P. Small-world networks and functional connectivity in Alzheimer's disease. Cerebral Cortex 2006;17(1):92–9.
Supekar K, Menon V, Rubin D, Musen M, Greicius MD. Network analysis of intrinsic functional brain connectivity in Alzheimer's disease. PLoS Computational Biology 2008;4(6):e1000100.